

Nowcasting transmission and suppression of the Delta variant of SARS-CoV-2 in Australia

Sheryl L. Chang¹, Oliver M. Cliff^{1,2}, Mikhail Prokopenko^{1,3}

¹ Centre for Complex Systems, Faculty of Engineering, The University of Sydney, Sydney, NSW 2006, Australia

² School of Physics, The University of Sydney, Sydney, NSW 2006, Australia

³ Sydney Institute for Infectious Diseases, The University of Sydney, Westmead, NSW 2145, Australia

Correspondence to:

Prof Mikhail Prokopenko, Centre for Complex Systems
Faculty of Engineering, University of Sydney, Sydney, NSW 2006, Australia
mikhail.prokopenko@sydney.edu.au

Summary

As of July 2021, there is a continuing outbreak of the B.1.617.2 (Delta) variant of SARS-CoV-2 in Sydney, Australia. The outbreak is of major concern as the Delta variant is estimated to have twice the reproductive number to previous variants that circulated in Australia in 2020, which is worsened by low levels of acquired immunity in the population. Using a re-calibrated agent-based model, we explored a feasible range of non-pharmaceutical interventions, in terms of both mitigation (case isolation, home quarantine) and suppression (school closures, social distancing). Our nowcasting modelling indicated that the level of social distancing currently attained in Sydney is inadequate for the outbreak control. A counter-factual analysis suggested that if 80% of agents comply with social distancing, then at least a month is needed for the new daily cases to reduce from their peak to below ten. A small reduction in social distancing compliance to 70% lengthens this period to over two months.

Introduction

Strict mitigation and suppression measures eliminated local transmission of SARS-CoV-2 during the initial pandemic wave in Australia (March–June 2020)¹, as well as a second wave that developed in the South Eastern state of Victoria (June–September 2020)^{2,3}. Several subsequent outbreaks were also detected and managed quickly and efficiently by contact tracing and local lockdowns, e.g., a cluster in the Northern Beaches Council of Sydney, New South Wales (NSW) totalled 217 cases and was controlled in 32 days by locking down only the immediately affected suburbs (December 2020–January 2021)⁴. Overall, the successful pandemic response was ensured by effective travel restrictions and social distancing, underpinned by comprehensive disease surveillance^{5,6,7,8,9}.

Unfortunately, the situation changed in mid-June 2021, when a highly transmissible variant of concern, B.1.617.2 (Delta), was detected. The first infection was recorded on June 16 in Sydney, and quickly spread through the Greater Sydney area. Within ten days, there were more than 100 locally acquired cumulative cases, triggering social distancing restrictions imposed in Greater Sydney and nearby areas¹⁰. By July 9 (23 days later), the locally acquired cases totalled 493⁴, and a tighter lockdown was announced¹⁰. The risk of a prolonged lockdown has become apparent¹¹, with no peak in incidence or prevalence confirmed at the time of writing.

The difficulty of controlling the outbreak is attributed to the high transmissibility of B.1.617.2 (Delta) variant, which is known to increase the risk of household transmission by approximately 60% in comparison to B.1.1.7 (Alpha) variant¹². This transmissibility is compounded by the low rate of vaccination in Australia, with around 6% the population fully vaccinated before the Sydney outbreak, and only 7.92% of Australians fully vaccinated by the end of June 2021¹³.

Several additional factors make the Sydney outbreak an important case study. Since previous pandemic waves were eliminated in Australia, the Delta variant has not been competing with other variants. This allows us to estimate its basic reproduction number R_0 in a cleaner setting. This transparency is further strengthened by low levels of acquired immunity to SARS-CoV-2 in the Australian population, given: (a) the pre-existing natural immunity is limited by cumulative confirmed cases of around 0.12%, and (b) immunity acquired due to vaccination is limited by vaccination coverage. Furthermore, the school winter break in NSW (28 June – 9 July) coincided with the period of social distancing restrictions announced on 26 June, with school premises remaining mostly closed beyond 9 July. Thus, the epidemic suppression policy of school closures is not a free variable, reducing the search-space of available control measures.

This study addresses several important questions. Firstly, we calibrate reproductive number R_0 and generation period T_{gen} of the Delta variant, using real-world data for an ongoing outbreak in Australia, in a transparent epidemiological setting. Secondly, in a nowcasting mode, we investigate a feasible range of key non-pharmaceutical interventions (NPIs): case isolation, home quarantine, school closures and social distancing, available to control the virus transmission within the population with a low acquired immunity. Finally, in a counter-factual mode, we quantify under what conditions the ongoing outbreak can be suppressed, aiming to provide actionable information on the extent of required NPIs, in comparison to previous pandemic control measures successfully deployed in Australia.

Methods

We utilised an agent-based model (ABM) for transmission and control of COVID-19 in Australia that has been developed in our previous work^{1,14} and implemented within a large-scale software simulator (AMTraC-19). The model was cross-validated with genomic surveillance data⁵, and contributed to social distancing policy recommendations broadly adopted by the World Health Organisation¹⁵. The model separately simulates each individual as an agent within a surrogate population composed of about 23.4 million software agents. These agents are stochastically generated to match attributes of anonymous individuals (in terms of age, residence, gender, workplace, susceptibility and immunity to diseases), informed by data from the Australian Census and the Australian Curriculum, Assessment and Reporting Authority. In addition, the simulator follows the known commuting patterns between the places of residence and work/study^{16,17,18}. Different contact rates specified within diverse social contexts (e.g., households, neighbourhoods, communities, and work/study environments) explicitly represent heterogeneous demographic and epidemic conditions. The model has previously been calibrated to produce characteristics of the COVID-19 pandemic corresponding to the ancestral lineage of SARS-CoV-2^{1,14}, using actual data from the first and second waves in Australia, and re-calibrated for B.1.617.2 (Delta) variant using incidence data of the Sydney outbreak (see Supplementary Material).

Each epidemic scenario is simulated by updating agents' states in discrete time. In this work we start from an initial distribution of infection, seeded by imported cases generated by the incoming international air traffic in Sydney's international airport (using data from the Australian Bureau of Infrastructure, Transport and Regional Economics)^{16,17}. At each time step during the seeding phase, this process probabilistically generates new infections within a 50 km radius of the airport, in proportion to the average daily number of incoming passengers (using a binomial distribution and data from the Australian Bureau of Infrastructure, Transport and Regional Economics)¹⁶.

A specific outbreak, originated in proximity of the airport, is traced over time by simulating the agents interactions within their social contexts, computed in 12-hour cycles ("day" and "night"). Once the outbreak size (cumulative incidence) exceeds a pre-defined threshold (e.g., 20 detected cases), the travel restrictions (TR) are imposed by the scenario, so that the rest of infections are driven by purely local transmissions, while no more overseas acquired cases are allowed (presumed to be in effective quarantine). Case-targeted non-pharmaceutical interventions (CTNPIs), such as case isolation (CI) and home quarantine (HQ), are applied from the outset.

The outbreak-growth phase can then be interrupted by another threshold (e.g., 100 cumulative detected cases) which triggers a set of general NPIs, such as social distancing (SD) and school closures (SC). Every intervention is specified via a macro-distancing level of compliance (i.e., $SD = 0.8$ means 80% of agents

Table 1: The macro-distancing parameters and interaction strengths: nowcasting (“now”) and counter-factual (“target”).

Strategy	Macro-distancing	Household	Interaction strengths	
	Compliance levels now → target		Community now → target	Workplace/School now → target
CI	0.7	1.0	0.25 → 0.1	0.25 → 0.1
HQ	0.5	2.0	0.25 → 0.1	0.25 → 0.1
SC (children)	1.0	1.0	0.5 → 0.1	0
SC (parents)	0.5	1.0	0.5 → 0.1	0
SD	0.4 → 0.8	1.0	0.25 → 0.1	0.1

are socially distancing), and a set of micro-parameters that indicate the level of social distancing within a specific social context (households, communities, workplaces, etc.). For instance, for those agents that are compliant, contacts (and thus likelihood of infection) can be reduced during a lockdown to $SD_w = 0.1$ within workplaces and $SD_c = 0.25$ within communities, whilst maintaining contacts $SD_h = 1.0$ within households.

Results

In order to model transmission of B.1.617.2 (Delta) variant during the Sydney outbreak of COVID-19 (June–July 2021), we re-calibrated the model to obtain the reproduction number approximately twice as high as our previous estimates for the two waves in Australia in 2020. In aiming at this level, we followed global estimates which showed that R_0 for B.1.617.2 is increased by 97% (95% CI of 76–117%) relative to the ancestral lineage¹⁹. The re-calibrated reproductive number was estimated as $R_0 \approx 6.09$ with 95% CI of 6.03–6.15. The corresponding generation period is estimated as $T_{gen} \approx 7.74$ with 95% CI of 7.68–7.81.

Using the ABM calibrated to B.1.617.2 (Delta) variant, we varied the macro- and micro-parameters (for CI, HQ, SC and SD), aiming to match the incidence data recorded during the Sydney outbreak in a *nowcasting* mode, i.e., up to the mid-July when the suppression was not yet achieved. The closest match to actual incidence data was produced by a moderate macro-level of social distancing compliance, $SD = 0.4$, see Fig. 1, and Supplementary Material for comparison with the corresponding growth rates. The considered SD levels were based on moderately reduced interaction strengths within community, i.e., $SD_c = 0.25$, see Table 1, which were inadequate for the outbreak suppression even with high macro-distancing such as $SD = 0.8$.

Furthermore, we considered feasible macro-levels of social distancing, $0.5 \leq SD \leq 0.9$, while maintaining $CI = 0.7$ and $HQ = 0.5$, in a *counter-factual* mode by varying the micro-parameters (interaction strengths for CI, HQ, SC and SD). This allowed us to simulate the outbreak suppression by reducing these levels within their feasible bounds. An eventual suppression of the outbreak is demonstrated only for macro-distancing at $SD \geq 0.7$, coupled with the lowest feasible interaction strengths for most interventions, i.e., $NPI_c = 0.1$ (where NPI is one of CI, HQ, SC and SD), as shown in Fig. 2 and summarised in Table 1. For $SD = 0.8$, new cases reduce below 10 per day approximately a month after a peak in incidence peak, while for $SD = 0.7$ this period exceeds two months. Social distancing at $SD = 0.9$ is probably infeasible, but would reduce the new cases to below 10 a day within three weeks following a peak in incidence.

Discussion

Despite a relatively high computational cost, and the need to calibrate numerous internal parameters, ABMs capture the natural history of infectious diseases in a good agreement with the established estimates of incubation periods, serial/generation intervals, and other key epidemiological variables. Various ABMs have been successfully used for simulating actual and counter-factual epidemic scenarios based on different initial conditions and intervention policies^{20,21,22,23}.

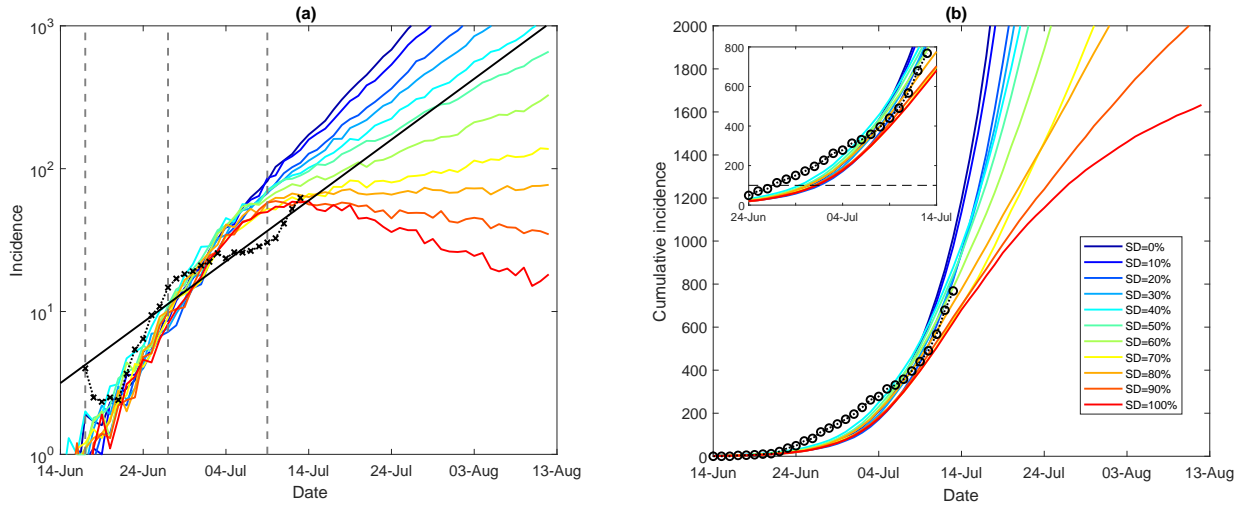


Figure 1: Nowcasting: a comparison between actual epidemic curves and nowcasting simulation scenarios. A moving average of the actual time-series for (a) (log-scale) incidence (crosses), and (b) cumulative incidence (circles); with an exponential fit of the incidence's moving average (black solid). Vertical dashed marks align the simulated days with the outbreak start (17 June, day 13), initial restrictions (27 June, day 23), and tighter lockdown (9 July, day 35). Traces corresponding to each social distancing (SD) compliance level are shown as average over 10 runs (coloured profiles). Each SD strategy, coupled with school closures, begins with the start of initial restrictions, when cumulative incidence exceeds 100 cases (b: inset). The alignment between simulated days and actual dates may slightly differ across separate runs. Case isolation and home quarantine are in place from the outset.

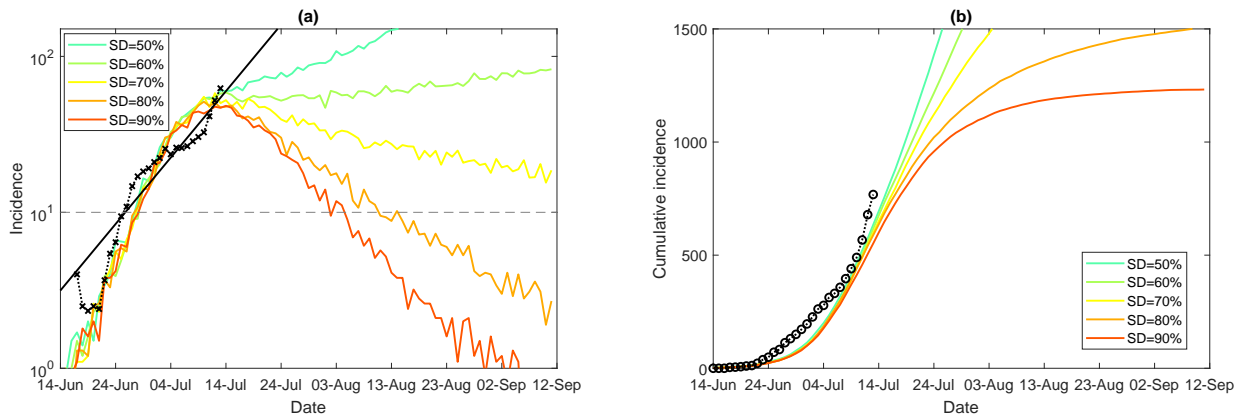


Figure 2: Suppression: a comparison between actual epidemic curves and counter-factual simulation scenarios. A moving average of the actual time-series for (a) (log scale) incidence (crosses), and (b) cumulative incidence (circles). Traces corresponding to each social distancing (SD) compliance level are shown as average over 10 runs (coloured profiles). Each SD strategy, coupled with school closures, begins with the start of initial restrictions (i.e., 27 June, simulated day 23), when cumulative incidence exceeds 100 cases. The alignment between simulated days and actual dates may slightly differ across separate runs. Case isolation and home quarantine are in place from the outset.

Our early COVID-19 study¹ modelled transmission of the ancestral lineage of SARS-CoV-2 characterised by the basic reproduction number of $R_0 \approx 3.0$ (adjusted $R_0 \approx 2.75$). This study compared several NPIs and identified the minimal SD levels required to control the first wave in Australia. Specifically, a compliance at the 90% level, i.e., $SD = 0.9$ (with $SD_w = 0$ and $SD_c = 0.5$) was shown to control the disease within 13-14 weeks. This relatively high SD compliance was required in addition to other restrictions (TR, CI, HQ), set at moderate levels of both macro-distancing ($CI = 0.7$ and $HQ = 0.5$), and interaction strengths: $CI_w = HQ_w = CI_c = HQ_c = 0.25$, $CI_h = 1.0$, and $HQ_h = 2.0$ ¹.

The follow-up work¹⁴ quantified possible effects of a mass-vaccination campaign in Australia, by varying the extents of vaccination coverage with different vaccine efficacy combinations. This analysis considered hybrid vaccination scenarios using two vaccines adopted in Australia: BNT162b2 (Pfizer/BioNTech) and ChAdOx1 nCoV-19 (Oxford/AstraZeneca). Herd immunity was shown to be out of reach even when a large proportion (82%) of the Australian population is vaccinated under the hybrid approach, necessitating future partial NPIs for up to 40% of the population. The model was also calibrated to the basic reproduction number of the ancestral lineage ($R_0 \approx 3.0$, adjusted $R_0 \approx 2.75$), and used the same moderate interaction strengths as the initial study¹ (except $SD_c = 0.25$, reduced to match the second wave in Melbourne in 2020).

In this work, we re-calibrated the ABM to incidence data from the ongoing Sydney outbreak driven by the Delta variant. The reproductive number was estimated to be at least twice as high ($R_0 \approx 6.09$) as the one previously estimated for pandemic waves in Australia. We then explored effects of available NPIs on the outbreak suppression. The nowcasting modelling identified that the current epidemic curves, which continue to grow (as of July 13), can be closely matched by moderate social distancing coupled with moderate interaction strengths within community ($SD = 0.4$, $SD_c = 0.25$), as well as moderate compliance with case isolation ($CI = 0.7$, $CI_w = CI_c = 0.25$) and home quarantine ($HQ = 0.5$, $HQ_w = HQ_c = 0.25$).

We note that the workers delivering essential services are exempt from lockdown restrictions. The fraction of the exempt population can be inferred conservatively as 4% (strictly essential)²⁴, more comprehensively as approximately 19% (including health care and social assistance; public administration and safety; accommodation and food services; transport, postal and warehousing; electricity, gas, water and waste services; financial and insurance services), but can reach more significant levels, around 33%, if all construction, manufacturing, and trade (retail/wholesale) are included in addition²⁵. The latter, broad-range, case limits feasible social distancing levels to approximately $SD \approx 0.7$. However, even with these inclusions, there is a discrepancy between the level estimated by ABM ($SD = 0.4$) and the broad-range feasible level ($SD \approx 0.7$). This discrepancy would imply that approximately 25-30% of the population have not been consistently complying with the imposed restrictions, while 30-35% may have been engaged in services deemed broadly essential (other splits comprising 60% of the “non-distancing” population are possible as well).

Such moderate level of compliance ($SD = 0.4$) would be inadequate for suppression of even less transmissible coronavirus variants¹. The Delta variant demands a stronger compliance and a reduction in the scope of essential services (especially, in a setting with low acquired immunity). Specifically, our results indicate that an effective suppression can be demonstrated only for the highest feasible compliance with social distancing ($SD \geq 0.7$), supported by dramatically reduced interaction strengths within the community and work/study environments ($NPI_c = NPI_w = 0.1$). Thus, the success can be achieved only in a combination of government actions (e.g., inclusion of some services currently deemed essential under the lockdown restrictions, while providing appropriate financial support to the affected businesses and employees), and a stronger community engagement with the suppression effort. Obviously, this challenge can be somewhat alleviated by a growing vaccination uptake. However, the vaccination rollout continues to be limited by various supply and logistics constraints. A failure in suppression of this growing outbreak, whether due to inadequate population compliance or a desire to maintain and restart socioeconomic activities, is likely to generate a substantial pandemic wave affecting the entire nation²⁶.

Study limitations

In modelling the Sydney outbreak we did not modify the incubation period, distributing it across the agents around mean 5.5 days. Recently, a shorter mean incubation period was reported for the Delta variant (4.4 days, with 95% CI of 3.9-5.0)²⁷. The sensitivity analysis¹ showed that the model is robust to changes

in the incubation period (e.g., the time to peak infectivity was investigated in the range between 4 and 7 days). As the epidemiology of the Delta variant continues to be refined with more data becoming available, our results may benefit from a retrospective analysis.

Another limitation is that the surrogate ABM population which corresponds to the latest available Australian Census data from 2016 (23.4M individuals, with 4.45M in Sydney) is smaller than the current Australian population (25.8M, with 4.99M in Sydney). This discrepancy is offset, however, by the outbreak size (three orders of magnitude smaller than Sydney population). Finally, the model does not directly represent in-hotel quarantine and in-hospital transmissions. Since the frontline professionals (health care and quarantine workers) were vaccinated in a priority phase carried out in Australia in early 2021, i.e., before the Sydney outbreak, this limitation has a minor effect.

Contributors

MP conceived and co-supervised the study and drafted the original Article. SLC and MP designed the computational experiments and re-calibrated the model. SLC carried out the computational experiments, verified the underlying data, and prepared all figures. All authors had full access to all the data in the study. All authors contributed to the editing of the Article, and read and approved the final Article.

Declaration of interests

We declare no competing interests.

Data sharing

No unique source code was developed for this project. The actual incidence data is available at: <https://www.covid19data.com.au/>. The ABM contact and transmission rates are detailed elsewhere¹⁶.

References

- [1] Chang SL, Harding N, Zachreson C, Cliff OM, Prokopenko M. Modelling transmission and control of the COVID-19 pandemic in Australia. *Nature Communications*. 2020;11(1):1–13.
- [2] Blakely T, Thompson J, Carvalho N, Bablani L, Wilson N, Stevenson M. The probability of the 6-week lockdown in Victoria (commencing 9 July 2020) achieving elimination of community transmission of SARS-CoV-2. *Medical Journal of Australia*. 2020;213(8):349–351.
- [3] Zachreson C, Mitchell L, Lydeamore MJ, Rebuli N, Tomko M, Geard N. Risk mapping for COVID-19 outbreaks in Australia using mobility data. *Journal of the Royal Society Interface*. 2021;18(174):20200657.
- [4] COVID-19 in Australia; 2021. Accessed on 10 July 2021. <https://www.covid19data.com.au/>.
- [5] Rockett RJ, Arnott A, Lam C, Sadsad R, Timms V, Gray KA, et al. Revealing COVID-19 transmission by SARS-CoV-2 genome sequencing and agent based modelling. *Nature Medicine*. 2020;26:1398–1404.
- [6] Scott N, Palmer A, Delpont D, Abeysuriya R, Stuart R, Kerr CC, et al. Modelling the impact of reducing control measures on the COVID-19 pandemic in a low transmission setting. *Medical Journal of Australia*. 2020;214(2):79–83.
- [7] Milne GJ, Xie S, Poklepovich D. A Modelling Analysis of strategies for relaxing COVID-19 social distancing. medRxiv. 2020.
- [8] Lokuge K, Banks E, Davis S, Roberts L, Street T, O’Donovan D, et al. Exit strategies: optimising feasible surveillance for detection, elimination, and ongoing prevention of COVID-19 community transmission. *BMC Medicine*. 2021;19(1):1–14.
- [9] Wilson N, Baker MG, Blakely T, Eichner M. Estimating the impact of control measures to prevent outbreaks of COVID-19 associated with air travel into a COVID-19-free country. *Scientific Reports*. 2021;11(1):1–9.
- [10] Health Protection NSW. COVID-19 in NSW – up to 8pm 9 July 2021; 2021. Accessed on 10 July 2021. <https://www.health.nsw.gov.au/Infectious/covid-19/Pages/stats-nsw.aspx>.
- [11] Chrysanthos, Natassia, The Age. ‘The length of this lockdown is up to each and every one of us’: Berejiklian; 2021. Accessed on 10 July 2021. <https://www.theage.com.au/national/australia-covid-news-live-sydney-braces-for-weeks-of-lockdown-pfizer-covid-19-vaccine-distribution-brought-forward-20210710-p588ig.html?post=p52gi7>.
- [12] Public Health England. Latest updates on SARS-CoV-2 variants detected in UK; 2021. Accessed on 11 June 2021. <https://web.archive.org/web/20210611115707/https://www.gov.uk/government/news/confirmed-cases-of-covid-19-variants-identified-in-uk>.
- [13] Australian Government, Department of Health. COVID-19 Vaccine Roll-out; 2021. Accessed on 1 July 2021. <https://www.health.gov.au/sites/default/files/documents/2021/07/covid-19-vaccine-rollout-update-1-july-2021.pdf>.

- [14] Zachreson C, Chang SL, Cliff OM, Prokopenko M. How will mass-vaccination change COVID-19 lockdown requirements in Australia? *The Lancet Regional Health – Western Pacific*. 2021:accepted; also: arXiv:2103.07061.
- [15] World Health Organization. Calibrating long-term non-pharmaceutical interventions for COVID-19: Principles and facilitation tools – Manila: WHO Regional Office for the Western Pacific; Strengthening the health systems response to COVID-19: Technical guidance # 2: Creating surge capacity for acute and intensive care, 6 April 2020 – Regional Office for Europe; 2020.
- [16] Cliff OM, Harding M, Piraveen M, Erten Y, Gambhir M, Prokopenko M. Investigating spatiotemporal dynamics and synchrony of influenza epidemics in Australia: an agent-based modelling approach. *Simulation Modelling Practice and Theory*. 2018;87:412–431.
- [17] Zachreson C, Fair KM, Cliff OM, Harding M, Piraveenan M, Prokopenko M. Urbanization affects peak timing, prevalence, and bimodality of influenza pandemics in Australia: results of a census-calibrated model. *Science Advances*. 2018;4:eaa5294.
- [18] Fair KM, Zachreson C, Prokopenko M. Creating a surrogate commuter network from Australian Bureau of Statistics census data. *Scientific Data*. 2019;6:150.
- [19] Campbell F, Archer B, Laurenson-Schafer H, Jinnai Y, Konings F, Batra N, et al. Increased transmissibility and global spread of SARS-CoV-2 variants of concern as at June 2021. *Eurosurveillance*. 2021;26(24):2100509.
- [20] Germann TC, Kadau K, Longini IM, Macken CA. Mitigation strategies for pandemic influenza in the United States. *Proceedings of the National Academy of Sciences*. 2006 Apr;103(15):5935–5940.
- [21] Ajelli M, Gonçalves B, Balcan D, Colizza V, Hu H, Ramasco JJ, et al. Comparing large-scale computational approaches to epidemic modeling: agent-based versus structured metapopulation models. *BMC Infectious Diseases*. 2010;10(1):1–13.
- [22] Nsoesie EO, Beckman RJ, Marathe MV. Sensitivity analysis of an individual-based model for simulation of influenza epidemics. *PLOS ONE*. 2012;7(10):0045414.
- [23] Zachreson C, Fair KM, Harding N, Prokopenko M. Interfering with influenza: nonlinear coupling of reactive and static mitigation strategies. *Journal of The Royal Society Interface*. 2020;17(165):20190728.
- [24] Wang W, Wu Q, Yang J, Dong K, Chen X, Bai X, et al. Global, regional, and national estimates of target population sizes for COVID-19 vaccination: descriptive study. *BMJ*. 2020;371.
- [25] Vandenbroek P. Snapshot of employment by industry, 2019; 2019. Accessed: July 10, 2021. https://www.aph.gov.au/About_Parliament/Parliamentary_Departments/Parliamentary_Library/FlagPost/2019/April/Employment-by-industry-2019.
- [26] Viana J, van Dorp CH, Nunes A, Gomes MC, van Boven M, Kretzschmar ME, et al. Controlling the pandemic during the SARS-CoV-2 vaccination rollout. *Nature Communications*. 2021;12(1):1–15.
- [27] Zhang M, Xiao J, Deng A, Zhang Y, Zhuang Y, Hu T, et al. Transmission Dynamics of an Outbreak of the COVID-19 Delta Variant B.1.617.2 – Guangdong Province, China, May–June 2021. *Chinese Center for Disease Control and Prevention*. 2021;3(27):584–586.
- [28] Efron B, Tibshirani RJ. An introduction to the bootstrap. vol. 57 of *Monographs on statistics and applied probability*. Chapman and Hall New York; 1994.
- [29] Ferretti L, Wymant C, Kendall M, Zhao L, Nurtay A, Abeler-Dörner L, et al. Quantifying SARS-CoV-2 transmission suggests epidemic control with digital contact tracing. *Science*. 2020;368(6491).
- [30] Wu JT, Leung K, Bushman M, Kishore N, Niehus R, de Salazar PM, et al. Estimating clinical severity of COVID-19 from the transmission dynamics in Wuhan, China. *Nature Medicine*. 2020;26(4):506–510.
- [31] Lauer SA, Grantz KH, Bi Q, Jones FK, Zheng Q, Meredith HR, et al. The incubation period of coronavirus disease 2019 (COVID-19) from publicly reported confirmed cases: estimation and application. *Annals of Internal Medicine*. 2020;172(9):577–582.
- [32] Centers for Disease Control and Prevention. Interim Guidance on Duration of Isolation and Precautions for Adults with COVID-19; 2020. <https://www.cdc.gov/coronavirus/2019-ncov/hcp/duration-isolation.html>.
- [33] Arons MM, Hatfield KM, Reddy SC, Kimball A, James A, Jacobs JR, et al. Presymptomatic SARS-CoV-2 infections and transmission in a skilled nursing facility. *New England Journal of Medicine*. 2020;382(22):2081–2090.
- [34] Wölfel R, Corman VM, Guggemos W, Seilmaier M, Zange S, Müller MA, et al. Virological assessment of hospitalized patients with COVID-2019. *Nature*. 2020;581(7809):465–469.
- [35] Bernal JL, Andrews N, Gower C, Gallagher E, Simmons R, Thelwall S, et al. Effectiveness of COVID-19 vaccines against the B.1.617.2 variant. *medRxiv*. 2021.
- [36] Harris RJ, Hall JA, Zaidi A, Andrews NJ, Dunbar JK, Dabrera G. Impact of vaccination on household transmission of SARS-CoV-2 in England. *medRxiv*. 2021.

Supplementary Material

Model calibration

Several internal parameters have been varied during calibration and sensitivity analyses^{1,14}, including

- the scaling factor $\kappa = 5.0$ which scales age-dependent contact and transmission rates to derive the reproductive number, estimated in this work using age-stratified weights as $R_0 \approx 6.09$ with 95% CI of 6.03–6.15 ($N = 6703$, randomly re-sampled in 100 groups of 100 samples; confidence intervals constructed by bootstrapping with the bias-corrected percentile method²⁸; R_0 adjusted by removing outliers is $R_0 \approx 5.56$);
- the fraction of symptomatic cases (set as 0.67 for adults, and 1/5 of that, i.e., 0.134, for children);
- different transmission probabilities for asymptomatic/presymptomatic and symptomatic agents: “asymptomatic infectivity” (factor of 0.5) and “pre-symptomatic infectivity” (factor of 1.0)^{29,30};
- incubation period, following log-normally distributed incubation times with mean 5.5 days (95%CI of 4.4–7.0 days)³¹;
- a post-incubation infectious asymptomatic or symptomatic period, between 7 and 14 days (uniformly distributed)^{32,33,34}; and
- different detection probabilities: symptomatic (detection per day is 0.23) and asymptomatic/pre-symptomatic (detection per day is 0.01)¹⁴.

Vaccination modelling

The national COVID-19 vaccine rollout strategy pursued by the Australian Government follows a hybrid approach combining two vaccines: BNT162b2 (Pfizer/BioNTech) and ChAdOx1 nCoV-19 (Oxford/AstraZeneca), administered across specific age groups, e.g., the Australians younger than 60 are generally eligible for the BNT162b2 vaccine. Our model accounts for differences in vaccine efficacy for the two vaccines approved for distribution in Australia, and distinguishes between separate vaccine components: efficacy against susceptibility (VEs), disease (VE_d) and infectiousness (VE_i). The extent of pre-outbreak vaccination coverage was set at 6% of the population, matching the level actually achieved in Australia by mid-June 2021

In setting the efficacy of vaccines against B.1.617.2 (Delta) variant, we followed the study of Bernal et al.³⁵ which estimated the efficacy of BNT162b2 (Pfizer/BioNTech) as VE_c \approx 0.9 (more precisely, 87.9%

with 95% CI: 78.2 to 93.2), and the efficacy of ChAdOx1 nCoV-19 (Oxford/AstraZeneca) as $VE_c \approx 0.6$ (i.e., 59.8% with 95% CI: 28.9 to 77.3). Given the constraint for the clinical efficacy¹⁴:

$$VE_c = VE_d + VE_s - VE_s VE_d, \tag{S1}$$

we set $VE_d = VE_s = 0.684$ for BNT162b2, and $VE_d = VE_s = 0.368$ for ChAdOx1 nCoV-19.

Recent studies also provided the estimates of efficacy against infectiousness (VE_i) for both considered vaccines at a level around 0.5³⁶. A general sensitivity analysis of the model to changes in VE_i and VE_c was carried out in¹⁴.

In both scenarios, the vaccinations are assumed to be equally balanced between the two vaccines, so that each type is given to approximately (i) 0.7M individuals, or (ii) alternatively, 2.1M individuals. Vaccines are distributed according to specific age-dependent allocation ratios, $\approx 2.457:30:1$, mapped to age groups $[\text{age} \geq 65] : [18 \leq \text{age} < 65] : [\text{age} < 18]$, as explained in our prior work¹⁴.

Growth rates

To estimate growth rates β , we fit a 7-day moving average of the corresponding incidence time-series $I(t)$ to an exponential function $\alpha \exp(\beta(t))$, using MATLAB R2020a function `movmean(I, [6 0])`. The growth rate of the observed incidence (for the time period between 17 June and 13 July inclusive) is estimated as $\beta = 0.098$, with 95% CI of 0.084–0.112. The growth rates for the time-series simulated for each SD level between 0.0 and 1.0 were estimated for the period between the simulated day corresponding to the lockdown start (27 June) until the end of simulation. These rates varied from $\beta_{0.0} = 0.138$, to $\beta_{1.0} = 0.003$, with $\beta_{0.3} = 0.099$ being the closest match to β , while $\beta_{0.4} = 0.084$ was within the range.